Recovery process of low-frequency fluctuations in laser diodes with external optical feedback

Yun Liu,[1] Peter Davis,[1] and Yoshiro Takiguchi[2]
[1]*ATR Adaptive Communications Research Laboratories, 2-2 Hikaridai, Seika-cho, Soraku-gun, Kyoto 619-0288, Japan*
[2]*Faculty of System Engineering, Shizuoka University, 3-5-1 Johoku, Hamamatsu 432-8561, Japan*
(Received 5 January 1999)

The recovery process of low-frequency fluctuations is experimentally investigated in a semiconductor laser with external optical feedback. Monotonic stepwise increase of the light output intensity is observed for various external cavity lengths. The time interval of each step corresponds to the round-trip time of the external cavity. Transitions between steps and dynamics within each step are analyzed. Experimental results are discussed with reference to the scenario of chaotic mode itinerancy. Statistical properties of time intervals between power dropout events are also discussed. [S1063-651X(99)05012-6]

PACS number(s): 05.45.−a, 42.55.Px, 42.65.Sf

I. INTRODUCTION

There has been some recent interest in the study of low-frequency fluctuations (LFF's) in laser diodes with external optical feedback. The phenomenon is characterized by an irregular oscillation whose frequency is much smaller than either relaxation oscillation or external cavity beat frequencies. Early research concentrated on experimental observations of power dropouts of laser output, measurements of distributions of the time interval between power dropout events, and parameter dependence of such measures [1,2]. Different explanations of the origin of LFF's have been proposed. One explanation used the Lang-Kobayashi rate equation of the single-mode model to describe the dynamics of LFF's and obtained a set of external cavity modes. Based on the mode distribution, it was interpreted that the power dropout occurs when a crisis arises between a local chaotic attractor and an antimode and the recovery process of LFF's as a result of chaotic itinerancy among external cavity modes [3,4]. Erratic picosecond pulsing of light intensity anticipated from the numerical model has been observed in experiment [5]. On the other hand, results of some recent experiments [6,7] suggested multimode operation of a laser accompanied with the occurrence of LFF's. Besides the above deterministic descriptions, descriptions based on stochastic origin have also been proposed. One stochastic scenario describes that lasers behave as an excitable medium and that LFF's are induced by noise [8,9]. The excitation model well accounted for the parameter dependence of the average time between dropout events in LFF's. Another stochastic model based on the analytic prediction of Henry and Kazarinov[10] provided an explanation for the experimental measurements of the statistical distribution of the time between dropout events and the dependence of the mean time on feedback strength [11]. However, further investigations are needed to clarify the mechanism for LFF's and distinguish between the different scenarios proposed so far.

This paper focuses on an experimental investigation of the recovery process of LFF's. Recently, Hegarty *et al.* [12] used a fast detector and a sampling oscilloscope to measure the averaged recovery dynamics. In this work, we vary the external cavity length from 30 cm to 10 m and compare recovery dynamics of different external cavity lengths. We use a detection system with a bandwidth up to 6 GHz. In particular, by setting a long external cavity length, we obtained a direct observation of the build-up process immediately after the power dropout. We found that the light intensity fluctuates around certain discrete levels during each round trip time in the recovery process. By averaging the time trace over multiple (usually about several thousand) power dropout events, a clear monotonic stepwise increase of light intensity is observed. The dependence of the average step width and average step number on bias injection current and external reflectivity is investigated. Dynamics within one step is dominated by relaxation oscillations. In the second part of this paper, we explain the recovery process of LFF's in terms of a transition among compound cavity modes. The comparison between the compound cavity mode distribution and experimental observations gives an intuitive interpretation about the stepwise increase of the light intensity in the recovery process of LFF's. Discussions on the validity of the single-mode model and the statistical property of power dropout events are also given.

II. EXPERIMENTAL RESULTS

Experiments are performed using a $Ga_xAl_{1-x}As$ laser diode (Sharp LT024) which lases in single mode with a wavelength of 782 nm at the threshold bias current of 43.9 mA [13]. Figure 1 shows the experimental setup of the laser with feedback. The temperature of the laser is stabilized to within about 0.05 °C. An external mirror of 95% reflectivity is placed at a distance from the laser output. This distance can be varied between 0.3 and 10 m. The light output is detected with a 6-GHz bandwidth photoreceiver (New Focus 1537). The signal is analyzed with a spectrum analyzer (22-GHz bandwidth) and a digital oscilloscope (LeCroy9362, 750 MHz analog bandwidth). Instead of a conventional neutral density (ND) variable attenuator, an acousto-optical modulator (AOM) is used to adjust the feedback strength. This is performed by directing the zeroth-order diffraction beam into the laser cavity and changing the diffraction ratio with the control signal. We have observed LFF's for different external cavity lengths. Figure 2 shows typical waveforms of LFF's for (a) $L_{\mathrm{ext}}=805$ cm and (b) $L_{\mathrm{ext}}=75$ cm, both at $I_b=45$ mA.

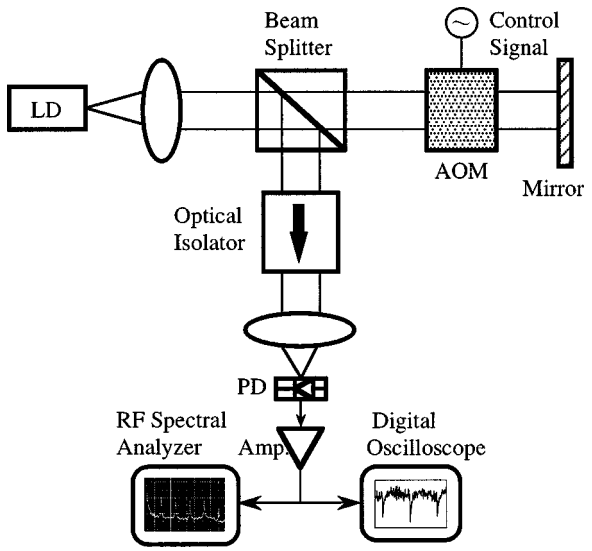

FIG. 1. Experimental setup for the observation of LFF's.

A. Monotonic stepwise increase of light intensity

To investigate the recovery process of LFF's, we trigger the oscilloscope at the power dropout and observe the time trace after the power dropout. Figure 3(a) shows a typical result for $L_{ext}=805$ cm. Fine structure of the dynamics within one round-trip time $\tau(=2L_{ext}/c=53.7$ ns) of the external cavity can be observed clearly by setting a long external cavity length. At the beginning of the recovery process in Fig. 3(a), one can easily recognize distinct steps of light intensity. To obtain a more clear image of the build-up process, we perform an averaging of time evolution over multiple power dropout events. This was easily performed with the oscilloscope since the trigger signal is very robust due to the sharpness of the power dropout. Figure 3(b) shows an averaged waveform of the build-up process as a result of a superposition of time traces for over 3000 events. The fast oscillations seen in Fig. 3(a) are washed out by the averaging process. In fact, the average waveform does not show significant change after averaging over several tens of waveforms. Figure 3(b) shows a very clear monotonic staircase of the light intensity. In each step, the average light intensity is locked to a certain level. It is found that the time duration of each step corresponds to the round-trip time of the external cavity.

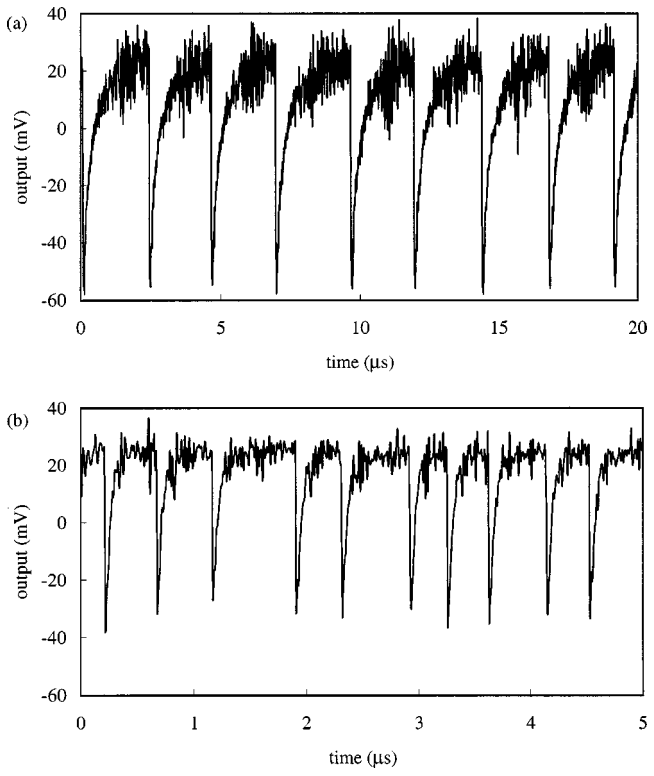

FIG. 2. Experimental time trace of LFF's for (a) $I_b=45$ mA, $L_{ext}=805$ cm, and (b) $I_b=45$ mA, $L_{ext}=75$ cm.

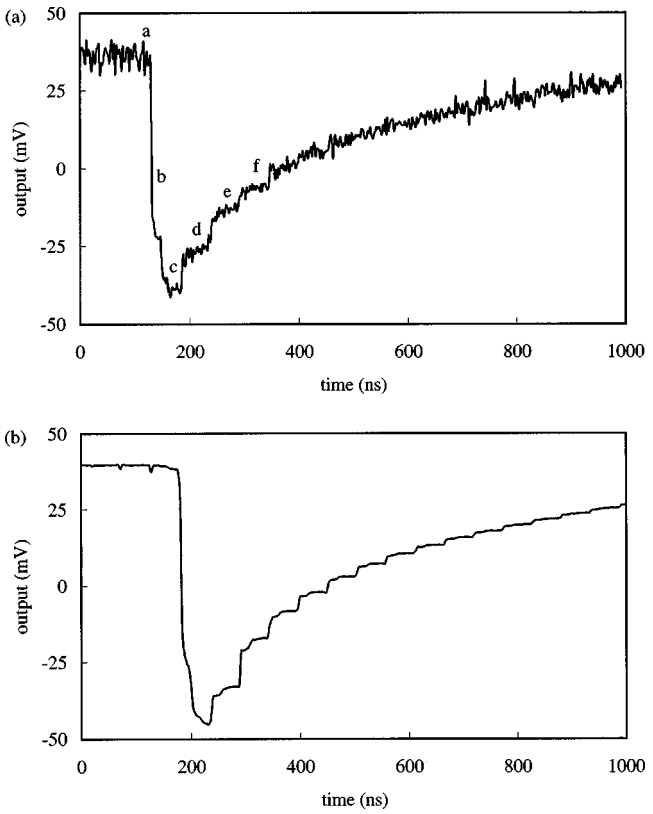

FIG. 3. (a) Single-shot time trace and (b) average time trace after power dropouts occur at $I_b=45$ mA and $L_{ext}=805$ cm. Notations $a-f$ in (a) are indicated for comparison with Fig. 8.

It might be argued that the above staircase of light intensity is only a property of the long external cavity. To answer this, we examined the averaged waveform for different external cavity lengths. Figure 4 depicts the results for the external cavity lengths at (a) $L_{ext}=600$ cm, (b) $L_{ext}=300$ cm, (c) $L_{ext}=150$ cm, and (d) $L_{ext}=75$ cm. We adjust the sampling time according to the external cavity length and normalize the light intensity variation since changing the external cavity length in the experiment inevitably changes the feedback strength and thus results in a variation of the oscillation amplitude. From these figures, we found that (i) a stepwise increase of light intensity exists in the recovery process of LFF's for all external cavity lengths, (ii) the duration time of each step corresponds to the round-trip time of the external cavity, (iii) the step difference gets smaller as the intensity increases, (iv) there appears in each step some high-frequency oscillation components which are not washed out

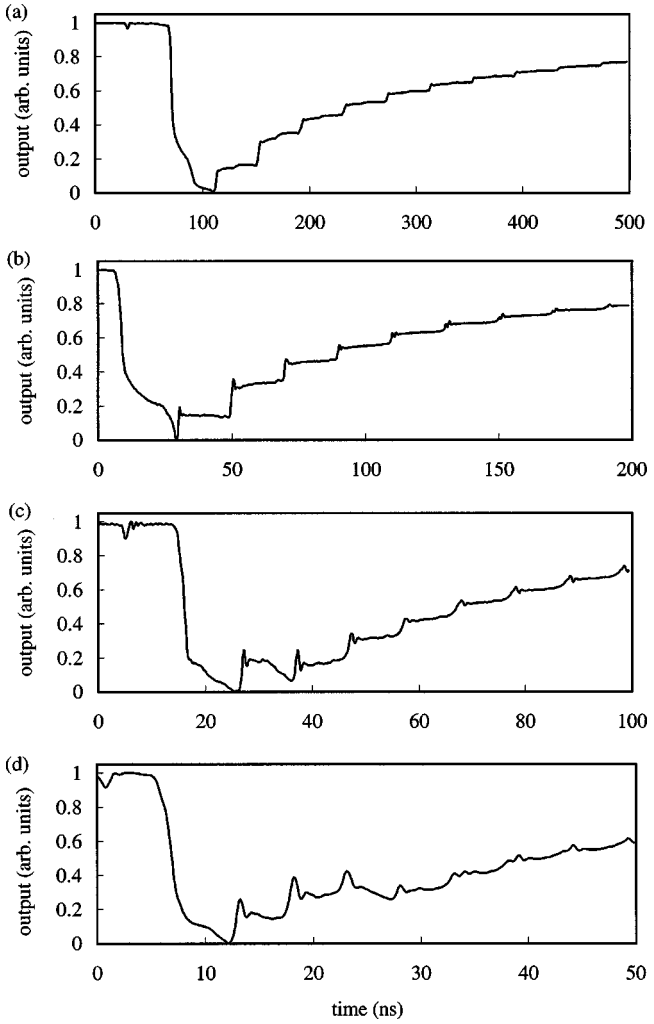

FIG. 4. Averaged time traces for different external cavity lengths at $I_b = 45$ mA. (a) $L_{ext} = 600$ cm, (b) $L_{ext} = 300$ cm, (c) $L_{ext} = 150$ cm, and (d) $L_{ext} = 75$ cm.

by averaging, and such high-frequency oscillation components become more noticeable for a short external cavity length.

B. Parameter dependence

When varying the bias injection current or external reflectivity while fixing the external cavity length, we observed the dependence of the recovery process on the parameters as follows.

(i) A stepwise increase of the light intensity is verified for all parameters as long as LFF is observed.

(ii) The step width corresponds to the round-trip time of the external cavity for all parameters.

(iii) The average time interval between consecutive power dropout events, expressed as number N_l of the round-trip time τ, depends on both the external reflectivity and the bias injection current, i.e., $N_l \propto \kappa$ and $N_l^{-1} \propto I_b$. N_l was calculated from a time trace with over 10^4 power dropout events. Figure 5(a) shows the variation of N_l versus the external reflectivity and Fig. 5(b) shows the variation of N_l versus the bias injection current. These results are consistent with previous works [1,2].

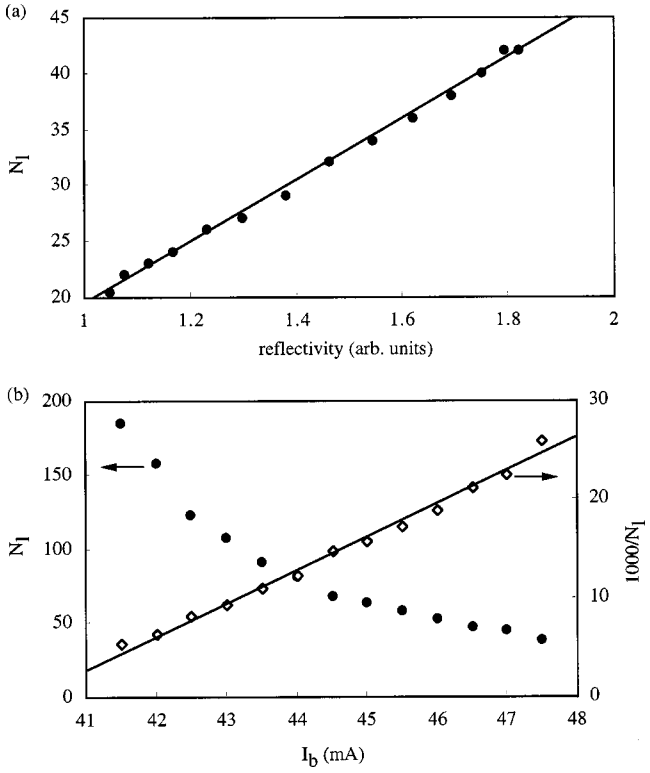

FIG. 5. Average step number (black circles) vs (a) external reflectivity at $I_b = 45$ mA, $L_{ext} = 805$ cm and (b) bias injection current at $L_{ext} = 805$ cm. Solid lines are fits to the data points. In (b), we also plot the inverse of the average step number as squares to show its linear dependence on the injection current. Solitary threshold is $I_{th} = 43.9$ mA.

(iv) The average step difference depends on the bias injection current and keeps almost constant when varying the feedback strength. The average step difference is calculated by dividing the power increase by the number of the steps. In Fig. 6, we show the step difference averaged over the first four steps immediately following the dropout as a function of the bias injection current.

C. High-frequency dynamics

Figure 7 shows some typical examples of single-shot waveforms of the recovery process for different parameter

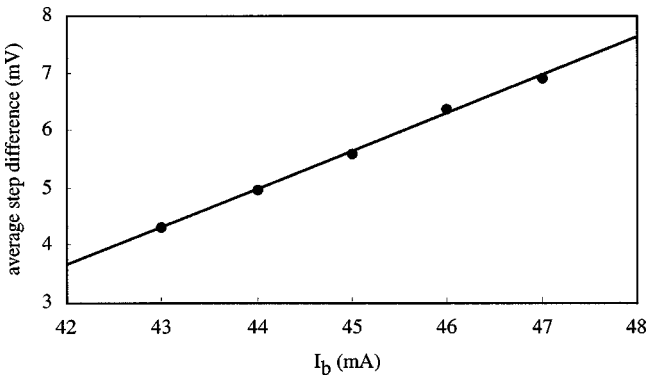

FIG. 6. Measured step difference (averaged over the first four steps immediately after the dropout) as a function of bias injection current at $L_{ext} = 805$ cm. Solid line is a fit to the data points. Solitary threshold is $I_{th} = 43.9$ mA.

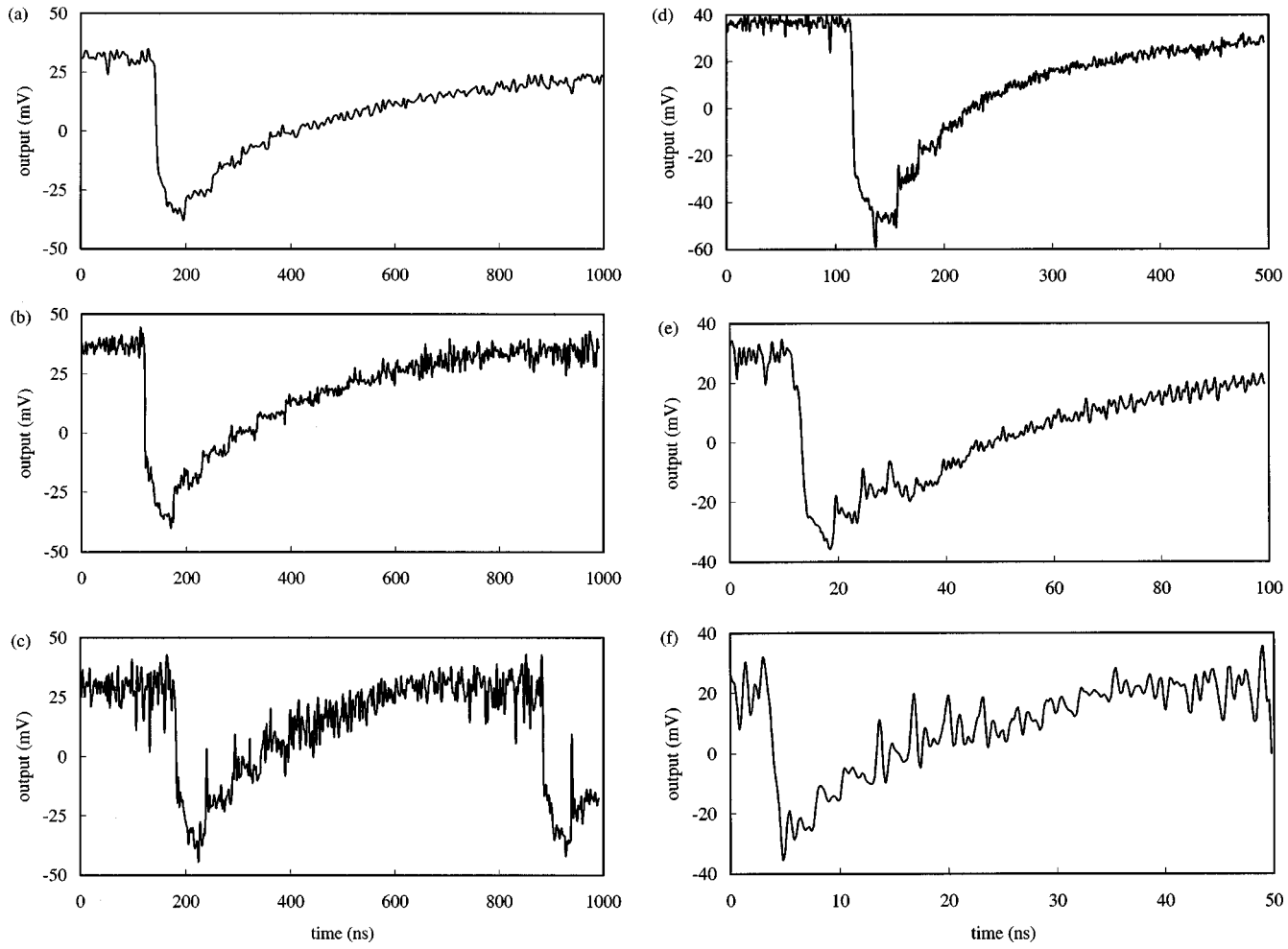

FIG. 7. High-frequency dynamics of LFF's for different parameter conditions. (a)–(c) Variations with bias injection current for $L_{ext}=805$ cm and feedback strength of -10.9 dB. (a) $I_b=44$ mA, (b) $I_b=46$ mA, (c) $I_b=47$ mA. Solitary threshold is $I_{th}=43.9$ mA. (d)–(f) Variations with external cavity length for $I_b=45$ mA. (d) $L_{ext}=300$ cm, (e) $L_{ext}=75$ cm, (f) $L_{ext}=45$ cm.

conditions. Waveforms corresponding to different bias injection current levels are plotted in (a) $I_b=44$ mA, (b) $I_b=46$ mA, and (c) $I_b=47$ mA at $L_{ext}=805$ cm, while waveforms for different external cavity lengths are plotted in (d) $L_{ext}=300$ cm, (e) $L_{ext}=75$ cm, and (f) $L_{ext}=45$ cm at $I_b=45$ mA.

The rf spectrum of the LFF oscillations showed three kinds of components: low-frequency power dropout events, the beats between external cavity modes, and high-frequency oscillations with frequency at or near the relaxation oscillation frequency. These three types of oscillations can be identified in the waveforms of Fig. 7. The amplitude of relaxation oscillations is enhanced as the injection current increases, as seen in Figs. 7(b) and 7(c). This enhancement was also observed in a recent experiment on the recovery process of LFF's for a short external cavity [12].

Several reports on high bandwidth observations of LFF's described the observation of high-frequency pulsing behavior [5,6]. Any such high-frequency oscillations would not be observed in Fig. 7 due to the bandwidth limitation of the oscilloscope. If we could repeat our experiment with a higher bandwidth, it is possible that what would be actually observed would be a steady increase in amplitude of high-frequency pulsing. In this case our results imply that there may be a stepwise increase in pulse amplitude. If pulsing is due to mode locking of compound cavity modes, a stepwise increase of the amplitude could be explained by discrete jumps of the center frequency of the compound cavity modes involved. We can speculate that even if high bandwidth measurements were made, discrete steps could still be seen in the recovery process after averaging over multiple power dropout events. Confirmation of this is left for future work.

III. DISCUSSION

A. Description of the recovery process based on compound cavity modes

The experimental observation of the stepwise increase in the light intensity suggests to us that it may be appropriate to attempt a description of the recovery process in terms of a sequence of transitions among compound cavity modes. First, we make the following hypotheses.

(i) In each step of the recovery process of LFF's, the laser is ''locked'' near a certain compound cavity mode. The light intensity fluctuates around a level which is characteristic of that mode.

(ii) The ''lock'' time is typically equal to the round-trip time of the external cavity. After this time the oscillation jumps to another mode.

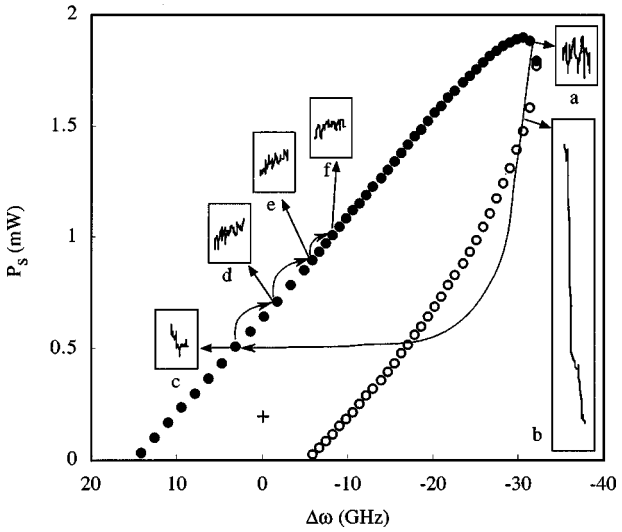

FIG. 8. Mode distribution diagram at the same parameter condition with Fig. 3. Black and white circles denote, respectively, compound cavity modes and antimodes. × denotes the fixed point for solitary laser. Horizontal axis is inverted for comparison with Fig. 3(a).

(iii) The sequence of steps in intensity seen in the recovery process is associated with an ordered sequence of compound cavity modes.

The recovery process of LFF's has been previously described as a sequence of transitions among compound cavity modes [3,4]. Specifically, LFF has been described as motion around the elliptical distribution of compound cavity modes obtained in a (Lang-Kobayashi) model of a single-mode laser with delayed optical feedback. Figure 8 shows the distribution of steady states of a single-mode laser with feedback, using parameters corresponding to the experimental results of Fig. 3. Details of the derivation of the modes are described in Appendix A. Since there are as many as several thousands of modes for the parameter condition of Fig. 3, only a subset of modes sampled at constant frequency intervals is plotted in Fig. 8. White circles indicate antimodes, which are always unstable, and black circles indicate modes which may be stable or unstable depending on the mode. A possible correspondence between the distribution of compound cavity modes obtained from the single-mode model and the recovery process of Fig. 3 according to the scenario of Refs. [3], [4] is indicated schematically by marking locations on the mode diagram with the insets of the waveforms from Fig. 3. Inset (b) corresponds to the collapse and insets (c), (d), (e), and (f) correspond to situations of locking to modes during the recovery process. This mode transition scenario suggests another hypothesis, as follows.

(iv) The typical step difference in terms of the frequency or the number of modes is a constant value which depends on the light intensity of the mode and the round-trip time, and a property of the mode such as the mode potential, which is discussed in Ref. [3], [14].

The preceding hypothesis is consistent with the fact that the intensity step difference gets smaller as the intensity increases. The experimental result that the average time between power dropout events is proportional to the feedback strength is also consistent with the scenario for recovery as a sequence of transitions in this model, since the number of modes increases with feedback strength, as can be seen in Eq. (A3) and (A4).

It is not clear how valid this single-mode scenario is for describing LFF's involving multiple modes. It has been shown that even if the laser without feedback lases in a single mode, LFF's in the presence of moderate optical feedback may involve multiple modes [6,7]. As pointed out in [6], oscillations in total intensity may be associated with out-of-phase oscillations of the multiple modes. However, so far there has been no specific dynamical model of multiple mode dynamics corresponding with experimental observations relating LFF's. According to theoretical models for a multimode laser diode with optical feedback, modes couple weakly through the depletion of the commonly shared carriers and the gain cross-saturation effect [15,16]. The coupling strength among different longitudinal modes is independent of the external feedback and is generally very weak compared with either the gain factor or the feedback effect. Therefore, we speculate that the compound mode distribution obtained from single-mode models might be regarded as a simplified representation of that for the multimode model, which provides a description of mode transitions. To further investigate the exact dynamic origin of the recovery process of LFF's, calculations based on the multimode model and comparison with the single-mode model are required. We should emphasize that the validity of hypotheses (i)–(iii) does not rely on the assumptions of the single-mode scenario.

B. Mean-time distribution of power dropout events

Since each power dropout event starts from a different initial condition, the actual step difference at each time is subject to fluctuations which may be both deterministic (chaos) and stochastic (Langevin origin). Here, we comment on whether a stochastic factor is required to account for the mean-time interval distribution of power dropout events. We divide time length into L subsets and define $P(m,L)$ as the probability density of the interval time between power dropouts in the mth$(0 \leqslant m \leqslant L)$ subset. Figure 9 shows histograms $P(m,L)$ for two typical LFF waveforms: (a) $L_{\mathrm{ext}} = 805$ cm and (b) $L_{\mathrm{ext}} = 75$ cm. Both plots are well approximated by a Poissonian distribution,

$$P(m,L) = \frac{L!}{m!(L-m)!}(\overline{m})^m(1-\overline{m})^{L-m}, \qquad (1)$$

where the value of the mean-time interval $L\overline{m}$ is calculated to be 6.2 for (a) and 3.3 for (b), which is shown by the solid line in each figure. It is verified that the power dropout in the light output of a laser diode with external feedback can be well identified by the Poissonian process with transition probability $p = \overline{m}$.

It is worthwhile to note that the distribution modeled by the Poissonian process does not necessarily mean it has a stochastic origin. For instance, the flip-flop process in the Lorenz model, which is absolutely deterministic, was also well modeled with the Poissonian process [17]. Therefore, numerical investigations of power dropout events for both noise-inclusion and noise-free models are needed to verify how stochastic factors affect the dynamic origin of LFF's.

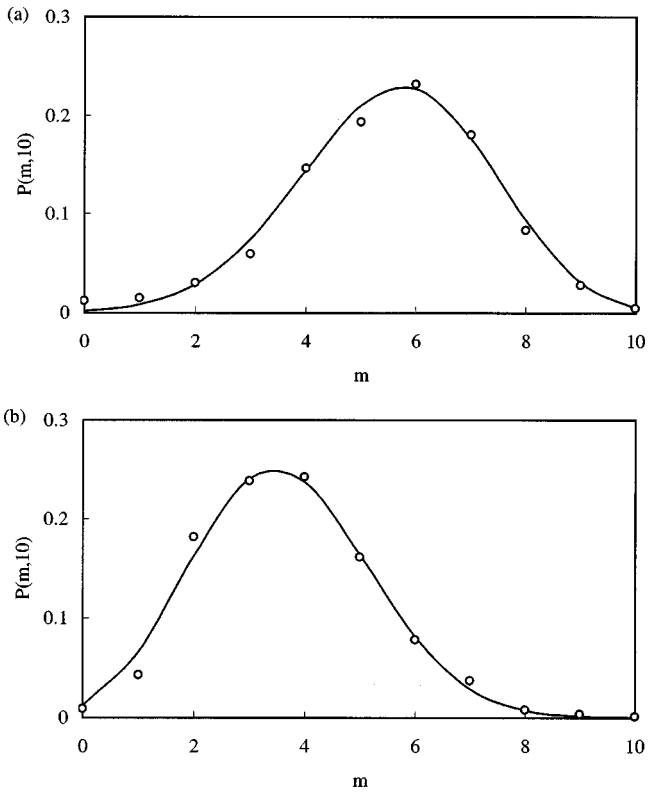

FIG. 9. Histograms of mean time interval (in unit of step width) between power drops for two typical LFF waveforms. (a) $I_b = 45$ mA, $L_{\text{ext}} = 805$ cm and (b) $I_b = 45$ mA, $L_{\text{ext}} = 75$ cm.

IV. CONCLUSION

In summary, we have experimentally investigated the recovery process of LFF's in a laser diode with external optical feedback using a detection system with a bandwith of 6 GHz. A clear monotonic stepwise increase of the light intensity was observed after the power dropout. The step width corresponds to the round-trip time of the external cavity. Step differences and average step number between power dropout events have been investigated as functions of bias injection current and feedback strength. High-frequency dynamics within each step is dominated by relaxation oscillations and such dynamics becomes undamped as the injection current increases or as the external cavity length decreases.

The stepwise increase of light intensity during the recovery process of LFF's has been interpreted in terms of a sequence of transitions among compound cavity modes. We suggest that the laser is ''locked'' to certain compound cavity modes during the recovery process. A comparison has been made between the experimental result of the recovery process and the mode distribution calculated from a single-mode Lang-Kobayashi rate equation, which showed an intuitive illustration about the staircase of the light intensity in the recovery process. Comments have been made on the validity of the single-mode model and the statistical property of power-dropout events.

ACKNOWLEDGMENTS

The authors are grateful to Professor J. Ohtsubo, Dr. N. Egami, and Dr. B. Komiyama for their helpful discussions and support.

APPENDIX A: COMPOUND CAVITY MODE DISTRIBUTION OF THE SINGLE-MODE LASER MODEL

To show how the stepwise increase of the light intensity is manifested in the compound cavity mode distribution, we numerically calculate the steady-state solutions of a laser diode with external optical feedback and derive its mode distribution. The dynamics of a single-mode laser diode with external optical feedback is written as a Lang-Kobayashi equation like [3,4]

$$\frac{dE(t)}{dt} = \frac{G_N}{2}(1+j\alpha)[N(t)-N_{\text{th}}]E(t) + \frac{\kappa}{\tau_{\text{in}}}E(t-\tau) + F_e(t), \tag{A1}$$

$$\frac{dN(t)}{dt} = J - \frac{N(t)}{\tau_s} - G_N[N(t)-N_0]|E(t)|^2 + F_N(t). \tag{A2}$$

Here, $E(t) = \sqrt{P(t)}\exp\{j[\omega_0 t + \varphi(t)]\}$ is the complex electric field of the optical field, P is the light intensity, φ is the phase, and ω_0 is the frequency of the solitary laser. Other parameters are as follows: N is the carrier number, N_{th} is the carrier number at the threshold, N_0 is the carrier number at transparency, and G_N, τ_{in}, and κ are, respectively, the gain coefficient, the round-trip time of the internal cavity, and the feedback strength.

Steady-state solutions ($P_s, N_s, \omega_s, \Delta N_s = N_s - N_{\text{th}}$, $\Delta\omega_s = \omega_s - \omega_0$) of the laser with optical feedback lie on an ellipse defined by

$$(\Delta\omega_s\tau_{\text{in}} - \alpha\tau_{\text{in}}G_N\Delta N_s/2)^2 + (\tau_{\text{in}}G_N\Delta N_s/2)^2 = \kappa^2, \tag{A3}$$

$$\Delta\omega_s\tau_{\text{in}} + \kappa\sin(\omega_s\tau + \tan^{-1}\alpha) = 0. \tag{A4}$$

We can further substitute the light intensity P_s instead of the carrier number N_s using $P_s = (J - N_s/\tau_s)/G_N(N_s - N_0)$ in Eq. (A3).

[1] M. Fujiwara, K. Kubota, and R. Lang, Appl. Phys. Lett. **38**, 217 (1981).
[2] J. Sacher, W. Elsässer, and E. O. Göbel, Phys. Rev. Lett. **63**, 2224 (1989).
[3] T. Sano, Phys. Rev. A **50**, 2719 (1994).
[4] G. H. M. van Tartwijk, A. M. Levine, and D. Lenstra, IEEE J. Sel. Top. Quantum Electron. **1**, 466 (1995).
[5] I. Fischer, G. H. M. Tartwijk, A. M. Levine, W. Elsässer, E. O. Göbel, and D. Lenstra, Phys. Rev. Lett. **76**, 220 (1996).
[6] G. Vaschenko, M. Giudici, J. J. Rocca, C. S. Menoni, J. R. Tredicce, and S. Balle, Phys. Rev. Lett. **81**, 5536 (1998).
[7] G. Huyet, S. Balle, M. Giudici, C. Green, G. Giacomelli, and J. Tredicce, Opt. Commun. **149**, 341 (1998).
[8] M. Giudici, C. Green, G. Giacomelli, U. Nespolo, and J. R.

Tredicce, Phys. Rev. E **55**, 6414 (1997).
[9] M. C. Eguia, G. B. Mindlin, and M. Giudici, Phys. Rev. E **58**, 2636 (1998).
[10] C. H. Henry and R. F. Kazarinov, IEEE J. Quantum Electron. **QE-22**, 294 (1986).
[11] A. Hohl, H. J. C. van der Linden, and R. Roy, Opt. Lett. **20**, 2396 (1995).
[12] S. P. Hegarty, G. Huyet, P. Porta, and J. G. McInerney, Opt. Lett. **23**, 1206 (1998).
[13] Y. Takiguchi, Y. Liu, and J. Ohtsubo, Opt. Lett. **23**, 1369 (1998).
[14] J. Mørk, M. Semkow, and B. Tromborg, Electron. Lett. **26**, 609 (1990).
[15] A. T. Ryan, G. P. Agrawal, G. R. Gray, and E. C. Gage, IEEE J. Quantum Electron. **QE-30**, 668 (1994).
[16] Y. Liu and P. Davis, Int. J. Bifurcation Chaos **8**, 1685 (1998).
[17] Y. Aizawa, Prog. Theor. Phys. **68**, 64 (1982).